J|A|C|S
ARTICLES
Published on Web 12/11/2002

Accurate First Principles Prediction of ^{17}O NMR Parameters in SiO_2: Assignment of the Zeolite Ferrierite Spectrum

Mickael Profeta,[†] Francesco Mauri,*[,†] and Chris J. Pickard[‡]

Contribution from the Laboratoire de Minéralogie-Cristallographie de Paris, Université Pierre et Marie Curie, 4, place Jussieu, 75252 Paris Cedex 5, France, and TCM Group, Cavendish Laboratory, Madingley Road, Cambridge CB3 OHE, United Kingdom

Received May 31, 2002; E-mail: Francesco.Mauri@lmcp.jussieu.fr

Abstract: ^{17}O NMR parameters, both the chemical shifts and the quadrupolar parameters, are calculated for SiO_2 polymorphs using density functional theory with the generalized gradient-corrected PBE functional. The gauge including projector augmented wave (GIPAW) method (Pickard, C. J.; Mauri, F. *Phys. Rev. B* **2001**, *63*, 245101) ensures the reproduction of all electron results while using computationally efficient pseudopotentials. The use of plane-waves permits fully converged calculations to be performed on structures containing 144 atoms in the unit cell, without the need to resort to the cluster approximation. The calculated NMR parameters of cristobalite, quartz, coesite, and faujasite are in excellent agreement with experimental data. This demonstrates that density functional theory is able to reproduce with high accuracy the ^{17}O NMR parameters in SiO_2 systems. This precision is used to assign the spectrum of the zeolite ferrierite. The data calculated for SiO_2 are used to confirm that no simple correlation between the chemical shift and *Cq* NMR parameters and Si−O−Si angle exists, emphasizing the importance of predictive theories in this field.

Introduction

Knowledge of the structure of silicate materials is important in many fields of materials science. The silicates cover a large range of materials from zeolites, minerals, and glasses to concretes, and generally have a complex structure, containing different cations or anions. In this contribution we will study pure tetrahedral SiO_2 structures, in which each silicon is contained in a SiO_4 tetrahedron and all oxygen atoms are linked by two silicon atoms. Crystalline examples of these systems are quartz, cristobalite, or coesite. Pure silica zeolites are also SiO_2 crystalline solids, but their structures contain large cavities where catalytic reactions can take place. Finally, amorphous silica is an example of a disordered tetrahedral SiO_2 system.

Solid-state nuclear magnetic resonance (NMR) spectroscopy is a powerful tool which probes the local structure around each atom in solid materials. For SiO_2 it is possible to study the local environment of silicon and oxygen atoms and to obtain information about the distances and angles between neighboring atoms.

^{29}Si solid-state NMR spectroscopy plays an important role in the characterization of silicate materials. For instance, it is a valuable tool in the determination of the connectivity of the SiO_4 tetrahedra. Furthermore, empirical rules that correlate the chemical shift to the Si−O−Si angles in silicate structures are now well established.[2]

^{17}O is a nucleus with a spin of $^5/_2$ for which it is possible to measure both the NMR chemical shift and the quadrupolar parameters. Moreover, the oxygen atoms are highly polarizable and in zeolites are the acid centers for catalytic reactions. For all these reasons, ^{17}O NMR has the potential to be a highly diagnostic probe for the study of zeolites. The understanding of ^{17}O NMR spectra is therefore of vital interest.

^{17}O solid-state NMR spectroscopy is a challenging technique due to the low natural abundance (0.037%) of this isotope and its low nuclear magnetic moment. Thanks to enriched samples and to the development of new high-resolution techniques, the amount of information available from ^{17}O spectra is rapidly increasing.[3−5] However, the spectra are still very difficult to interpret as no empirical rules have yet been found to enable the assignment of the peaks and to obtain structural information for each site.

Under these circumstances, first principles calculations can be extremely helpful for the understanding of NMR spectra. An accurate calculation of the NMR parameters would allow us to separate and to assign the contributions of the oxygen sites present in the structure. Information about the structure of these sites could also then be extracted. This will make finding any empirical correlations easier and lead to the understanding of new ^{17}O spectra.

[†] Université Pierre et Marie Curie.
[‡] Cavendish Laboratory.

(1) Pickard, C. J.; Mauri, F. *Phys. Rev. B* **2001**, *63*, 245101.
(2) Mauri, F.; Pasquarello, A.; Pfrommer, B. G.; Yoon, Y. G.; Louie, S. G. *Phys. Rev. B* **2000**, *62*, R4786−R4789.
(3) Grandinetti, P. J.; Baltisberger, J. H.; Farnan, I.; Stebbins, J. F.; Werner, U.; Pines, A. *J. Phys. Chem.* **1995**, 99, 12341−12348.
(4) Bull, L. M.; Bussemer, B.; Anupold, T.; Reinold, A.; Samoson, A.; Sauer, J.; Cheetham, A. K.; Dupree, R. *J. Am. Chem. Soc.* **2000**, *122*, 4948−4958.
(5) Bull, L. M.; Cheetham, A. K.; Anupold, T.; Reinold, A.; Samoson, A.; Sauer, J.; Bussemer, B.; Lee, Y.; Gann, S.; Shore, J.; Pines, A.; Dupree, R. *J. Am. Chem. Soc.* **1998**, *120*, 3510−3511.

10.1021/ja027124r CCC: $25.00

The first calculations of NMR parameters were performed with quantum chemistry codes using atomic orbital bases. These codes perform calculations for molecules and can only model solids within the cluster approximation. A cluster is a molecule with the same local structure as the solid, where the atom to be studied is placed at the center of the structure. As NMR is a local spectroscopy, if the cluster is large enough, calculations should give the same result as in the full solid. However, using quantum chemical methods, it is difficult to reach full convergence both with respect to the atomic basis set and to the cluster size. It has been reported that only qualitative results can be achieved.[4−6] These qualitative results are sufficient for solids where the shifts for the oxygen sites are well separated, by more than 3 or 4 ppm, as in coesite,[3] or in the faujasite zeolite.[5] However, they are not sufficient for a structure such as the ferrierite dealluminated zeolite, where the oxygen chemical shifts are separated by less than 1 ppm. To quote from the paper of Bull et al.[4] "[...] theoretical predictions of the chemical shifts, quadrupolar coupling constants and asymmetry parameters show only qualitative agreement with the experimental ^{17}O NMR spectra [...] Higher accuracy is required from the shift calculations [to assign the experimental spectra] which is currently not possible."

Recently, two of us have developed a method to calculate chemical shifts within periodic boundary conditions and the pseudopotential approximation.[1] In this method, we extend the projector augmented wave (PAW) method of Blöchl[7] to the calculation of the all-electron magnetic response using the gauge-including projector augmented wave (GIPAW) method. Thanks to this method, it is now possible to calculate fully converged chemical shifts in solids without resorting to the cluster approximation. In this contribution we apply the GIPAW method to the calculation of the ^{17}O chemical shifts in several SiO_2 polymorphs and two zeolites. Moreover, we adapt Petrilli and Blöchl's method[8] for the calculation of the all-electron electric field gradient. We can therefore also compute the quadrupolar parameters of ^{17}O spectra for the same systems.

1. Definitions, Numerical Methods, and Technical Details

In the present work, we consider all the SiO_2 crystalline structures for which the ^{17}O NMR parameters have thus far been measured, namely α-cristobalite, α-quartz, coesite, and the all-silica zeolites ferrierite and faujasite. The unit cells of these structures contain 12, 9, 24, 108, and 144 atoms, respectively. We compute all the ^{17}O NMR parameters and the ^{29}Si chemical shifts.

An applied external magnetic field **B** induces a nonuniform magnetic field $\mathbf{B}_{in}(\mathbf{r})$. The NMR shielding tensor, $\vec{\sigma}(\mathbf{r})$ is defined as the ratio between $\mathbf{B}_{in}(\mathbf{r})$ and **B**:

$$\mathbf{B}_{\mathrm{in}}(\mathbf{r}) = -\vec{\sigma}(\mathbf{r})\mathbf{B}. \tag{1}$$

The isotropic shielding $\sigma(\mathbf{r})$ is one-third of the trace of $\vec{\sigma}(\mathbf{r})$. The isotropic chemical shift $\delta(\mathbf{r})$ for a nucleus in the position **r** is defined as:

$$\delta(\mathbf{r}) = -[\sigma(\mathbf{r}) - \sigma^{\mathrm{ref}}] \tag{2}$$

where σ^{ref} is the isotropic shielding of the same nucleus in a reference system. For ^{17}O and ^{29}Si, the references are a spherical liquid water sample and a tetramethylsilane sample, respectively.

The ^{17}O quadrupolar coupling constant Cq and the asymmetry parameter η are obtained from the traceless electric field gradient tensor (EFG) $\vec{G}(\mathbf{r})$:

$$G_{\alpha\beta}(\mathbf{r}) = \frac{\partial E_\alpha(\mathbf{r})}{\partial r_\beta} - \frac{1}{3}\delta_{\alpha\beta}\sum_\gamma \frac{\partial E_\gamma(\mathbf{r})}{\partial r_\gamma} \tag{3}$$

where α,β,γ denote the Cartesian coordinates x, y, z and $E_\alpha(\mathbf{r})$ is the local electric field at the position **r**, which can be calculated from the charge density $n(\mathbf{r})$:

$$E_\alpha(\mathbf{r}) = \int d^3r' \frac{n(\mathbf{r}')}{|\mathbf{r}-\mathbf{r}'|^3}(r_\alpha - r'_\alpha) \tag{4}$$

The EFG tensor is then equal to:

$$G_{\alpha\beta}(\mathbf{r}) = \int d^3r' \frac{n(\mathbf{r}')}{|\mathbf{r}-\mathbf{r}'|^3}\left[\delta_{\alpha\beta} - 3\frac{(r_\alpha - r'_\alpha)(r_\beta - r'_\beta)}{|\mathbf{r}-\mathbf{r}'|^2}\right] \tag{5}$$

If we label the eigenvalues of the EFG tensor V_{xx}, V_{yy}, V_{zz} so that $|V_{zz}| > |V_{yy}| > |V_{xx}|$, then

$$Cq = \frac{eQV_{zz}}{h} \tag{6}$$

and

$$\eta = \frac{V_{xx} - V_{yy}}{V_{zz}} \tag{7}$$

where e is the absolute value of the electron charge, h is the Planck constant, and Q is the nuclear quadrupolar momentum.

In our calculations we obtain absolute shielding tensors. To fix the ^{29}Si scale, we choose $\sigma^{\mathrm{ref}} = 337.3$ ppm, in such a way that the experimental and theoretical $\delta(\mathbf{r})$ of quartz coincide. Given the larger experimental uncertainty in the ^{17}O chemical shifts, for the ^{17}O scale we choose σ^{ref} in such a way that the sum of all experimental $\delta(\mathbf{r})$ considered in this work coincides with the corresponding sum of theoretical values. The resulting σ^{ref} for ^{17}O is 262.6 ppm. Finally, to compute the quadrupolar coupling constant Cq of ^{17}O we use the experimental value of $2.55\ 10^{-30}$ m^2 for the constant Q.[9] Note that in other calculations on SiO_2, a smaller value of Q of $2.23\ 10^{-30}$ m^2 is required to fit the theoretical results to the experimental data.[4,6]

The calculations are performed within density functional theory (DFT). Among the generalized gradient approximations (GGA), PW91 is found to give the best results for chemical shift calculations for light elements.[10,11] Here we use the PBE generalized gradient approximation,[12] which gives results very similar to those obtained with PW91 and corrects some

(6) Xue, X.; Kanzaki, M. *Solid State Nucl. Magn. Res.* **2000**, *16*, 245−259.
(7) Blöchl, P. E. *Phys. Rev. B* **1994**, *50*, 17953.
(8) Petrilli, H. M.; Blöchl, P. E.; Blaha, P.; Schwarz, K. *Phys. Rev. B* **1998**, *57*, 14690.
(9) Pyykkö, P. *Mol. Phys.* **2001**, *99*, 1617−1629.
(10) Malkin, V. G.; Malkina, O. L.; Salahub, D. R. *Chem. Phys. Lett.* **1993**, *204*, 80−95.
(11) Cheeseman, J. R.; Trucks, G. W.; Keith, T. A.; Frisch, *J. Chem. Phys.* **1996**, *104*, 14.
(12) Perdew, J. P.; Burke, K.; Ernzerhof, M. *Phys. Rev. Lett.* **1996**, *77*, 3865.

numerical instabilities of the PW91 functional. The core-valence interactions are described by norm-conserving pseudopotentials[13] in the Kleinman−Bylander[14] form, with *s* nonlocality for O and *s* and *p* nonlocality for Si. The cores of Si and O are $1s^2 2s^2 2p^6$ and $1s^2$, respectively. The eigenfunctions of the pseudo-Hamiltonian coincide with the corresponding all-electron wave function only beyond a core radius r_c. Indeed, the pseudo-wave functions are chosen to be as smooth as possible in the core region, and the correct nodal structure of the wave functions is lost.[13] In our work the core radii of Si and O are equal to 1.7 and 1.5 au respectively. We describe the crystalline structures as infinite periodic solids using periodic boundary conditions. The wave functions are expanded in plane waves with a kinetic energy smaller than the cutoff energy (E_{cut}) of 80 Ry, which corresponds to a number of plane waves per SiO_2 unit ranging from 3000 to 6000, depending on the density. In particular, in the faujasite calculation we use a basis set containing 300 000 plane waves. The integrals over the Brillouin zone are done using a single Baldereschi point[15] for faujasite, and using a Monkhorst−Pack k-point grid[16] for the other samples. A $4 \times 4 \times 4$ grid is used for cristobalite and quartz, a $2 \times 2 \times 2$ grid for coesite, and a $4 \times 2 \times 1$ grid for ferrierite.

The use of pseudopotentials in NMR calculations is not trivial. Indeed, the NMR parameters are dominated by the regions near the core where the pseudo- and true wave functions differ. Here we compute the shielding tensors using the GIPAW approach.[1] In GIPAW the all-electron induced current is reconstructed from the pseudo-wave functions. This permits the reproduction of the results of a fully converged all-electron calculation.[1] The periodic boundary conditions are implemented in GIPAW following ref 17. To compute the EFG tensors, we use PAW with an approach similar to that described in ref 8. The details of our implementation are reported in the appendix. For the PAW and GIPAW calculations we use two projectors in each *s* and *p* angular momentum channel for O, and in the *s*, *p*, and *d* channel for Si.

The NMR calculations are performed with the experimental geometries determined by X-ray or neutron diffraction.[18−22] In our tables the O sites are described using the notation of these experimental works. Since the internal positions of ferrierite have been debated,[4] and two distinct experimental geometries are available in the literature,[21,23] we optimize the ferrierite structure by DFT in the local density approximation. We use the experimental lattice parameters, rescaled by −0.3% to take into account the systematic error of LDA in the Si−O bond length, and we optimize the internal parameters. The NMR calculations and the diffraction patterns have been computed with the theoretical internal coordinates and the experimental lattice vectors. The theoretical internal coordinates, reported in Table 1, are close to that of ref 21. Indeed the powder diffraction patterns of the theoretical and experimental structure,[21] simulated with the XND Rietveld code,[24] can be hardly distinguished (see Figure 1).

Table 1. Fractional Atomic Coordinates of the Ferrierite Structure Obtained after Relaxation[a]

atom	sof	*x*	*y*	*z*	atom	sof	*x*	*y*	*z*
Sil	0.5	0.00000	0.50000	0.15266	O12	1.0	0.1758	0.4888	0.2018
Si2	1.0	0.29228	0.50005	0.27343	O15	1.0	-0.0206	0.4089	0.1027
Si3	1.0	0.21867	0.30150	0.33213	O22	0.5	0.5000	0.5000	0.2509
Si4	1.0	0.30623	0.20661	0.18173	O23	1.0	0.2516	0.4139	0.3269
Si5	1.0	0.00856	0.29933	0.08306	O24	1.0	0.2439	0.5961	0.3149
					O34	1.0	0.2881	0.2518	0.2599
					O43	1.0	0.3292	0.2594	0.3983
					O35	1.0	0.5097	0.2190	0.1557
					O45	1.0	0.1774	0.2593	0.1266
					O55	0.5	0.0494	0.2889	0.0000

[a] The lattice parameters were not relaxed; $a = 741.8$ pm, $b = 1407.0$ pm, and $c = 1871.3$ pm. The symmetry of the crystal was also constrained to be orthorhombic *Pnnm*, and sof stands for the site occupation factor.

We use the PARATEC[25] code for the NMR calculations and the CPMD[26] code for the ferrierite geometry optimization. We also use Gaussian98[27] to compute the NMR absolute shieldings on a small cluster.

For the GIPAW NMR calculations we use a parallel IBM Power4 (1.3 GHz) computer. The calculation of all the NMR parameters requires 10 h on 16 processors for ferrierite, and 12 h on 32 processors for faujasite.

2. Convergence Tests and Absolute Shieldings

Before presenting the results for the SiO_2 structures, we show that the parameters described in the previous section and used in the rest of the report are appropriate for accurate calculations. Using plane waves, it is straightforward to verify the convergence of the calculation with respect to the basis set. Indeed, a single parameter, the cutoff energy E_{cut}, fixes the number of basis functions per unit volume. The required number of plane waves depends critically on the pseudopotential core radius r_c of the smallest element in the calculation, in our case O. The larger r_c is the smaller the E_{cut} can be. However, the pseudo-wave functions coincide with the true wave functions only beyond r_c. Thus, the core region cannot be arbitrarily large, otherwise the chemical bonding will not be correctly described. In Table 2 we present the theoretical results for the ^{17}O σ and Cq, and the ^{29}Si σ for cristobalite and quartz as a function of the O r_c and E_{cut}. The results obtained with the values described

(13) Troulier, N.; Martins, J. L. *Phys. Rev. B* **1991**, *43*, 1993.
(14) Kleinman, L.; Bylander, D. *Phys. Rev. Lett.* **1982**, *48*, 1425.
(15) Baldereschi, A. *Phys. Rev. B* **1973**, 7, 5212−5215.
(16) Monkhorst, H. J.; Pack, J. D. *Phys. Rev. B* **1976**, *13*, 5188.
(17) Mauri, F.; Pfrommer, B. G.; Louie, S. G. *Phys. Rev. Lett.* **1996**, *77*, 5300.
(18) Schmahl, W. W.; Swainson, I. P.; Dove, M. T.; Graeme-Barber, A. *Z. Kristallogr.* **1992**, *201*, 125−145.
(19) Will, G.; Belletto, M.; Parrish, W.; Hart, M. *J. Appl. Crystallogr.* **1988**, *21*, 182.
(20) Geisinger, K. L.; Spackman, M. A.; Gibbs, G. V. *J. Phys. Chem.* **1987**, *91*, 3237.
(21) J. E. Lewis, J.; Freyhardt, C. C.; Davis, M. E. *J. Phys. Chem.* **1996**, *100*, 5039−5049.
(22) Hriljac, J. A.; Eddy, M. M.; Cheetham, A. K.; Donohue, J. A.; Ray, G. A. *J. Solid State Chem.* **1993**, *106*, 66−72.
(23) Morris, R. E.; Weigel, S. J.; Henson, N. J.; Bull, L. M.; Janicke, M. T.; Chmelka, B. F.; Cheetman, A. K. *J. Am. Chem. Soc.* **1994**, *116*, 11849−11855.
(24) Berar, J.-F.; Baldinozzi, G. 1998; http://www-cristallo.polycnrs-gre.fr/xnd/.
(25) Pfrommer, B.; Raczkowski, D.; Canning A.; Louie, S. G. *PARATEC* (PARAllel Total Energy Code); Lawrence Berkeley National Laboratory (with contributions from Mauri, F.; Cote, M.; Yoon, Y.; Pickard, C.; Haynes, P.) for more information see www.nersc.gov/proj ects/paratec.
(26) Hutter, J.; Ballone, P.; Bernasconi, M.; Focher, P.; Fois, E.; Goedecker, S.; Marx, D.; Parrinello, M.; Tuckerman, M. CPMD, version 3.3.5, MPI für Festkörperforschung and IBM Research Laboratory 1990−1998.
(27) Frisch, M. J.; Trucks, G. W.; Schlegel, H. B.; Scuseria, G. E.; Robb, M. A.; Cheeseman, J. R.; Zakrzewski, V. G.; Montgomery, J. A., Jr.; Stratmann, R. E.; Burant, J. C.; Dapprich, S.; Millam, J. M.; Daniels, A. D.; Kudin, K. N.; Strain, M. C.; Farkas, O.; Tomasi, J.; Barone, V.; Cossi, M.; Cammi, R.; Mennucci, B.; Pomelli, C.; Adamo, C.; Clifford, S.; Ochterski, J.; Petersson, G. A.; Ayala, P. Y.; Cui, Q.; Morokuma, K.; Malick, D. K.; Rabuck,A. D.; Raghavachari, K.; Foresman, J. B.; Cioslowski, J.; Ortiz, J. V.; Baboul, A. G.; Stefanov, B. B.; Liu, G.; Liashenko, A.; Piskorz, P.; Komaromi, I.; Gomperts, R.; Martin, R. L.; Fox, D. J.; Keith, T.; Al-Laham, M. A.; Peng, C. Y.; Nanayakkara, A.; Gonzalez, C.; Challacombe, M.; Gill, P. M. W.; Johnson, B. G.; Chen, W.; Wong, M. W.; Andres, J. L.; Head-Gordon, M.; Replogle, E. S.; Pople, J. A. *Gaussian 98*, revision A.9; Gaussian Inc.: Pittsburgh, PA, 1998.

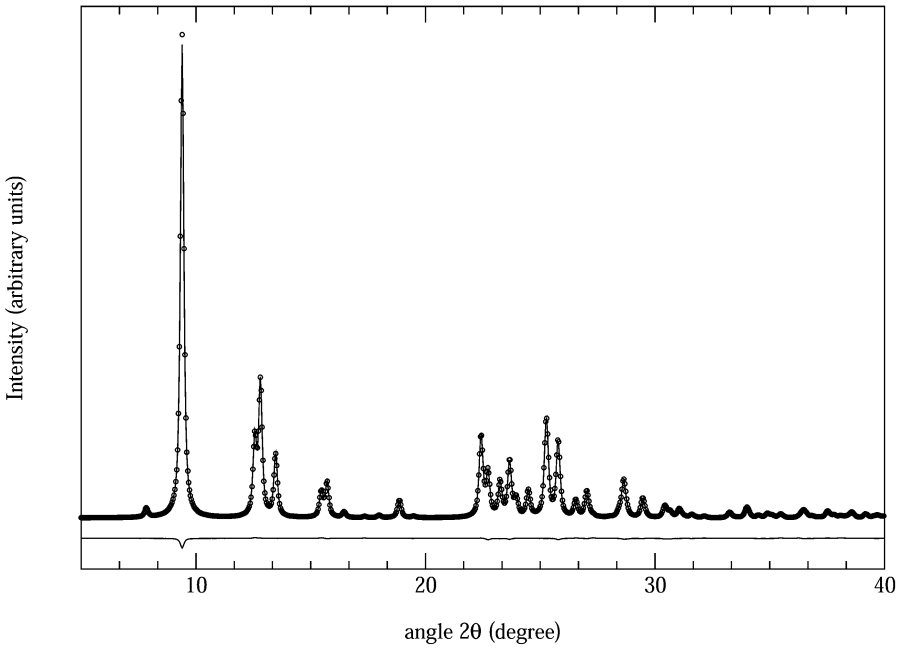

Figure 1. Calculated X-ray diffraction patterns using the experimental (line) and relaxed (circle) atomic positions. The difference between them is represented in the bottom at the same scale.

Table 2. Convergence of the Calculated ^{17}O ^{29}Si NMR Parameters for Cristobalite and Quartz[a]

		cristobalite			quartz		
r_c	energy	*Cq*	^{17}O σ	^{29}Si σ	*Cq*	^{17}O σ	^{29}Si σ
1.3	60	5.09	229.06	444.98	5.10	224.20	443.05
	80	5.27	222.17	444.96	5.28	217.25	443.02
	100	5.28	222.34	444.95	5.30	217.39	443.01
	120	5.27	223.19	444.95	5.28	218.26	443.01
1.5	60	5.28	223.59	446.42	5.28	218.71	444.47
	80	5.31	222.17	446.38	5.33	217.26	444.42
	100	5.31	222.91	446.39	5.33	218.02	444.43
	120	5.31	223.24	446.37	5.33	218.35	444.42
Exp.		5.21	270.7	477.0	5.19	267.1	475.6

[a] r_c is the core radius of the O pseudopotential in atomic units and "energy" is the cut-off energy of the plane waves in Rydbergs. The experimental values are taken from ref 30 for *Cq*. The experimental absolute shieldings are calculated from the absolute shielding of a reference, gas water, as measured in ref 31 for ^{17}O, and SiH4, as measured in ref 32 for ^{29}Si and from the experimental chemical shift δ reported in Table 4.

in the previous section and used in the rest of the report ($r_c = 1.5$ au and $E_{cut} = 80$ Ry), are very close to those obtained with the smallest core radius and the largest basis set ($r_c = 1.3$ au and $E_{cut} = 120$ Ry). In particular the relative chemical shifts between cristobalite and quartz computed with the two sets of parameters are practically identical. Note also that there is a large but systematic error between theory and experiment in the absolute shieldings. This is not a problem as the calculations reproduce the relative chemical shifts well.

Finally we verify that our results, obtained with plane-waves and pseudopotentials, reproduce well those obtained with the more conventional all-electron quantum-chemical approaches as implemented in Gaussian98.[27] We consider a small $O-(SiH_3)^2$ cluster extracted from the α-quartz structure. The cluster is saturated with H and the Si−H bond lengths are fixed to 1.483 Å. Since the PBE functional is not available in Gaussian98, we use the LDA and PW91 functionals. The Gaussian98 σ are computed using the gauge including atomic orbitals (GIAO) and the individual gauges for atoms in molecules (IGAIM) methods.[28,29] In Table 3 we present the results of the ^{17}O and ^{29}Si σ as a function of the DFT functional, the basis set and the computational approach. At the LDA level, the results obtained with the largest basis set (cc-pCV5Z), are very close to those obtained with GIPAW. The larger difference observed in the GGA ^{29}Si results is probably due to the use of different GGA functionals. For reference we also include the results obtained with GIAO and the IGLO-III basis, which have been used in previous NMR calculations on zeolites.[4,5]

Table 3. NMR Absolute Shieldings for a $O-(SiH_3)_2$ Cluster Derived from the α-Quartz Structure[a]

basis	method	DFT	^{17}O σ	$^{29}Si(1)$ σ	$^{29}Si(2)$ σ
IGLO−III	GIAO	LDA	319.50	351.59	350.21
cc-pCVDZ	IGAIM	LDA	307.78	372.57	370.92
cc-pCVTZ	IGAIM	LDA	315.09	345.48	344.06
cc-pCVQZ	IGAIM	LDA	317.67	341.84	340.45
cc-pCV5Z	IGAIM	LDA	316.49	340.98	339.60
plane-waves	GIPAW	LDA	315.05	345.55	344.18
cc-pCV5Z	IGAIM	PW91	313.07	364.48	363.16
plane-waves	GIPAW	PBE	313.26	374.94	373.62

[a] The O−Si(1) distance is shorter than the O−Si(2) distance. We use a cc-pCVxZ basis for both O and Si. For H we use the corresponding cc-pVxZ basis. We have obtained the Si cc-pCVxZ basis from Peterson.[33] In the plane-waves calculation we use a cubic supercell with a 13.3 Å lattice constant, a pseudopotential core radius of 1.3 au for O, and a 120 Ry plane-wave energy cutoff.

3. Results for the SiO_2 Structures

Our theoretical ^{17}O results for the SiO_2 structures are collected in Table 4, along with the corresponding experimental data. To interpret the experimental NMR spectra and to verify the agreement between theory and experiment, it is necessary to assign the experimental ^{17}O peaks to the different crystallographic sites. This assignment can easily be performed for the zeolite faujasite[5] by comparing the theoretical and experimental

(28) Ditchfield, R. *J. Chem. Phys.* **1972**, *56*, 5688.
(29) Keith, T. A.; Bader, R. F. W. *Chem. Phys. Lett.* **1992**, *194*, 1.

Table 4. Experimental and Theoretical ^{17}O NMR Parameters[a]

		experiment					theory			
	ref	*I*	δ	*Cq*	η	site	*I*	δ	*Cq*	η
coesite	3	0.83	29	6.05	0.000	O1	1	25.8	6.24	0.040
		1.05	41	5.43	0.166	O2	1	39.2	5.56	0.190
		2.05	57	5.45	0.168	O3	2	56.0	5.45	0.190
		2.16	53	5.52	0.169	O4	2	52.4	5.73	0.166
		1.90	58	5.16	0.292	O5	2	57.8	5.23	0.296
cristobalite	30		37.2	5.21	0.13			39.3	5.30	0.145
quartz	30		40.8	5.19	0.19			44.3	5.31	0.202
ferrierite	4	0.56	43.1	5.62	0.10	O34	1	42.1	5.55	0.07
		1.00	41.6	5.22	0.10	O23	1	41.3	5.20	0.15
		1.00	40.7	5.35	0.10	O12	1	40.0	5.47	0.07
		0.71	39.6	5.29	0.15	O22	0.5	39.3	5.31	0.11
		0.71	39.0	5.38	0.15	O24	1	38.1	5.43	0.06
		1.00	37.0	5.27	0.20	O35	1	36.9	5.35	0.17
		1.00	37.0	5.32	0.20	O43	1	37.1	5.20	0.21
		1.00	35.9	5.46	0.20	O15	1	35.8	5.47	0.11
		1.00	34.8	5.64	0.20	O45	1	32.7	5.67	0.05
		0.56	28.0	5.57	0.20	O55	0.5	28.2	5.54	0.12
faujasite	5	1	47.3	5.14	0.1	O3	1	48.6	5.08	0.16
		1	42.3	5.10	0.3	O1	1	44.3	5.09	0.26
		1	37.2	5.39	0.2	O2	1	38.3	5.33	0.27
		1	34.8	5.28	0.2	O4	1	36.8	5.32	0.18

[a] *I* represents the relative intensity of each peak, δ the chemical shift relative to water in ppm, *Cq* the quadrupolar coupling in MHz and η the asymmetry parameter. The NMR parameters are computed at the experimental geometries in all systems but ferrierite, for which we use the theoretically relaxed structure.

^{17}O chemical shifts, which are very well spaced. In coesite, the assignment requires, in addition, the use of the parameter η to discriminate the two sites with the close experimental δ of 57 and 58 ppm. The agreement between the experimental and theoretical ^{17}O NMR parameters in faujasite and coesite, is excellent. In particular, the spacing between chemical shifts within each of these two structures is much better reproduced by our calculations than by previous calculations.[5,6] This improvement can be attributed to the use in refs 5 and 6 of the cluster or the Hartree−Fock (HF) approximation.

The assignment in ferrierite is more complex, given that there are 10 inequivalent O sites, nine of which are clustered within a small δ range of 8 ppm. Indeed the accuracy of previous NMR calculations has proven to be insufficient to assign the spectra.[4] To accomplish this task we take advantage of both the *Cq* and δ parameters and the improved accuracy of our theoretical predictions. The EFG anisotropy is not useful because of the large experimental uncertainty in η for ferrierite. In Figure 2, we present, in a two-dimensional (δ,*Cq*) space, the measured and computed NMR parameters for each O site of ferrierite. We assign the experimental spectra by minimizing the following quantity:

$$\chi^2 = \frac{1}{2N-1}\sum_{i=1}^{N}\left[\frac{(\delta_i^{\mathrm{exp}} - \delta_i^{\mathrm{th}} + c)^2}{2\Delta\delta^2} + \frac{(Cq_i^{\mathrm{exp}} - Cq_i^{\mathrm{th}})^2}{2\Delta Cq^2}\right] \quad (8)$$

as a function of *c* and the assignment, where the parameter *c* is introduced to account for an eventual error in the determination of the ^{17}O chemical shift scale (see discussion below), *N* is the number of sites, the superscript distinguishes experimental and theoretical quantities, and $\Delta\delta$ and ΔCq are the declared uncertainties in the experimental results, equal to 0.3 ppm and 0.03 MHz.

If we compute the ^{17}O parameters using the experimental ferrierite geometry, we obtain an optimal χ^2 of 3.1. To check

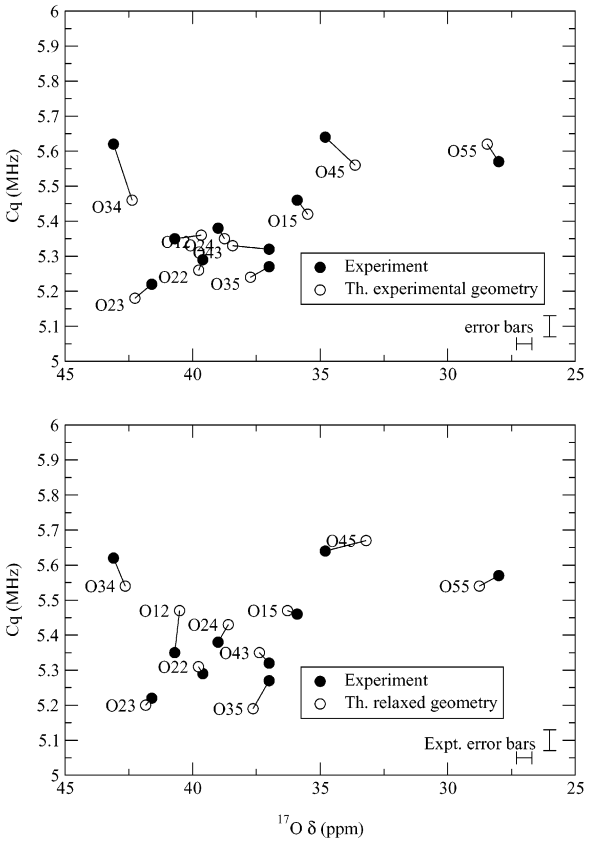

Figure 2. Each ^{17}O site in the ferrierite structure is represented by a point whose coordinates are its *Cq* and **5** parameters. The theoretical chemical shifts are translated so that their mean values coincide with the experimental ones. The NMR parameters are computed in the upper panel with the experimental geometry and in the lower panel with the relaxed geometry.

the influence of the crystal geometry, we recompute the NMR parameters with the theoretically relaxed structure (Table 1). The relaxation modifies the ^{17}O parameters, but the assignment remains unchanged, with a reduced χ^2 of 2.2. The reduced χ^2 suggests that the relaxed geometry is more accurate than the experimental one. It is interesting to note that NMR is much more sensitive to the geometry than the X-ray diffraction. Indeed the NMR parameters obtained with the two geometries are clearly different, as shown in Figure 2, whereas the simulated powder diffraction patterns (Figure 1) are practically identical. The next three best assignments after the optimal one, computed on the relaxed structure, have a χ^2 of 2.7, 3.2, and 3.2. These three assignments are obtained from the optimal one by the O43 ↔ O35, the O22 ↔ O24, and the O22 ↔ O12 permutation, respectively.

There is a discrepancy between theoretical and experimental intensities in ferrierite, see Table 4. There are four experimental peaks with intensities close to 1/2 instead of the two expected from the crystal structure, which suggests that this problem is related to the measurements or to the ^{17}O enrichment.[4]

Once the experimental peaks are assigned, we can plot in Figure 3 the calculated δ values against the experimental ones. The agreement between theory and experiment is very good, since the least-squares correlation line computed on all data has a slope of 1.007 and a correlation coefficient of 0.981. In particular, if we consider the structures with more than one inequivalent O site (coesite, ferrierite, and faujasite), the points within the same structure are even better aligned on lines with

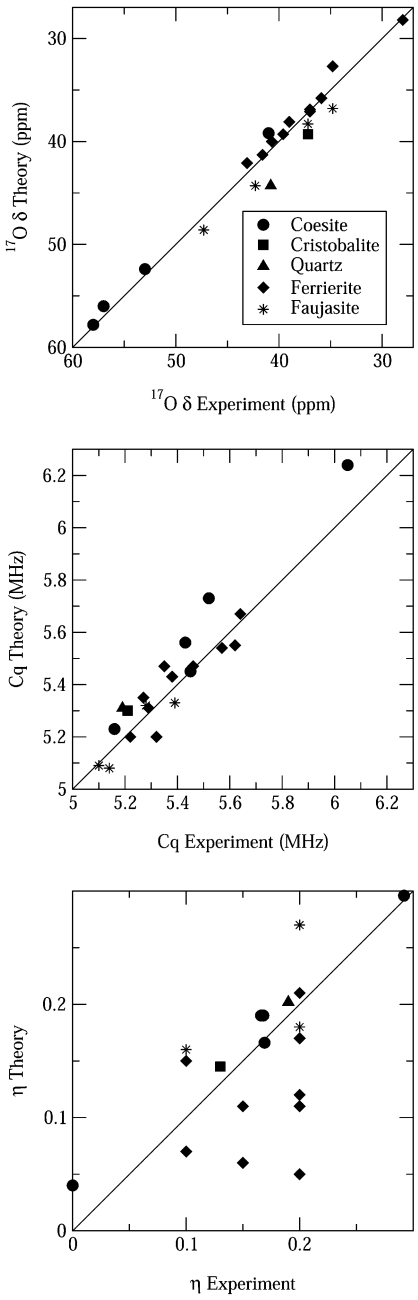

Figure 3. The calculated ^{17}O parameters of Table 4 are plotted against the experimental data. The line represents the perfect correspondence between calculation and experiment.

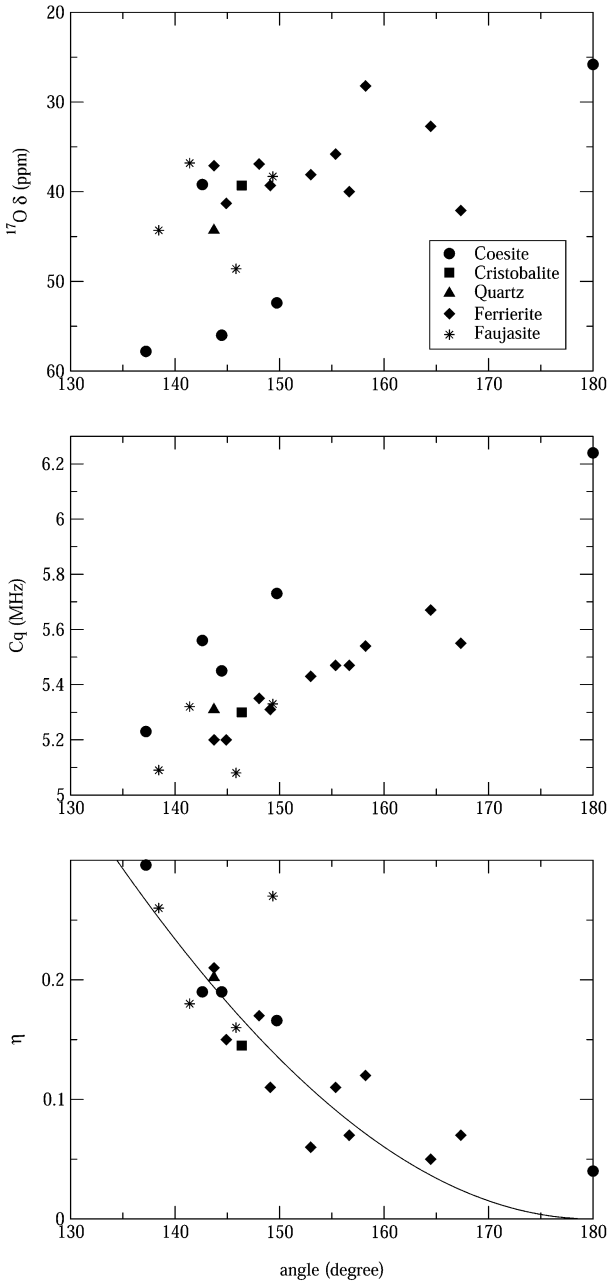

Figure 4. Theoretical ^{17}O NMR parameters of Table 4 are plotted as a function of the local Si−O−Si angle. In the lower panel, we show the line of the empirical correlation proposed in ref 36, $\eta = 1 + \cos(\text{angle})$.

slope 1, with a small nonzero intercept at the origin. However, in quartz, in which a single O site is present, the discrepancy between theory and experiment for the ^{17}O δ is equal to 3.5. This discrepancy is much larger than those observed in the description of the spacings between the chemical shifts of inequivalent sites of coesite, ferrierite, and faujasite. These observations could indicate a reference problem in the ^{17}O chemical shift scale in the different experiments.

In Figure 3 we also compare the experimental and theoretical *Cq* and η parameters. For *Cq* the calculations reproduce closely the measurements. The agreement between theory and experiments is apparently less good for η. This is not surprising given the large experimental error bars (of the order of 0.05 to 0.1) on this quantity for ferrierite and faujasite.

It is tempting to look for correlations between the NMR ^{17}O parameters and the local structure. A correlation between Si−O−Si angle and ^{29}Si chemical shifts is, indeed, well-known,[34] and similar correlations have been sought for ^{17}O,[3,4,35] without clear evidence. In Figure 4, we plot δ, *Cq* and η as a function of the angle Si−O−Si. Even if a general trend is visible, it is clear that δ and *Cq* are not just simple functions of the Si−O−Si angle, θ. The best linear correlations between δ

(30) Pedro, D.; Farnan, I. Unpublished results.
(31) Wasylishen, R. E.; Mooibroek, S.; Macdonald, J. B. *J. Chem. Phys.* **1984**, *81*, 1057.
(32) Jameson, C. J.; Jameson, A. K. *Chem. Phys. Lett.* **1988**, *149*, 300.
(33) Peterson, K.; T. H. Dunning, J. *J. Chem. Phys.* Manuscript submitted.
(34) Smith, J. V.; Blackwell, C. S. *Nature* **1983**, *303*, 223.
(35) Freude, D.; Loeser, T.; Michel, D.; Pingel, U.; Prochmow, D. *Solid State Nucl. Magn. Res.* **2001**, *20*, 46−60.

Table 5. Experimental and Theoretical ^{29}Si NMR Chemical Shifts[a]

	experiment			theory	
	I	δ	site	*I*	δ
coesrite	1	−113.9	Si1	1	−114.69
	1	−108.1	Si2	1	−108.41
cristobalite		−108.5			−109.05
quartz		−107.1			−107.1
ferrierite	1	−116.5	Si1	1	−117.67
	2	−112.3	Si2	2	−113.66
	2	−111.9	Si3	2	−112.23
	2	−117.2	Si4	2	−119.45
	2	−116.2	Si5	2	−116.29
faujasite		−107.8			−106.69

[a] *I* represents the relative intensity of each peak, δ the chemical shift relative to tetramethylsilane in ppm. The NMR parameters are computed at the experimental geometries in all systems but ferrierite, for which we use the theoretically relaxed structure. The experimental data are taken from refs. 21, 34.

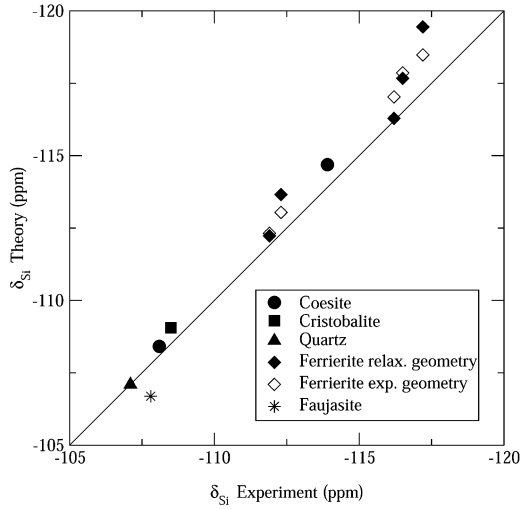

Figure 5. Calculated ^{29}Si chemical shifts are plotted against experimental data. The line represents the perfect correspondence between calculation and experiment. For ferrierite we report the results obtained with both the experimental and relaxed geometry.

and *Cq* and cos(θ) are, $\delta = 97.52 + [66.38 \cos(\theta)]$ and $Cq = 3.215 - [2.576 \cos(\theta)]$. The absolute values of the correlation coefficient are low, 0.60 and 0.73, respectively. In contrast the EFG asymmetry parameter η is better correlated with cos(θ), the correlation coefficient being 0.85. The best linear correlation is $\eta = 0.89 + [0.85 \cos(\theta)]$, which is very close to the $\eta = 1 + \cos(\theta)$ correlation proposed in ref 36 and reported in Figure 4. Unfortunately η is the parameter which is the most difficult to extract accurately from experiments.

Finally in Table 5 and Figure 5, we compare the theoretical and experimental ^{29}Si chemical shifts. In this case, the linear-regression correlation coefficient (computed for all the data of Table 5) is 0.988 a value close to that obtained for the ^{17}O δ. However, the ^{29}Si linear-regression slope is 1.153, that is, the spacings between chemical shifts are overestimated by the PBE-GGA functional.

Conclusions

In conclusion, we have shown that density functional theory, within the generalized gradient-corrected PBE approximation is able to reproduce with high accuracy the ^{17}O NMR parameters in the SiO_2 systems. We have used the GIPAW and the PAW methods, which reproduce all electron results while using computationally efficient pseudopotentials. We have eliminated the need of a cluster approximation by adopting periodic boundary conditions. Finally, the efficiency of the pseudopotential plane wave approach has allowed us to perform calculations, which are fully converged with respect to the basis set, on zeolites containing 144 atoms in the unit cell. The accuracy of our theoretical predictions has been used to assign, for the first time, the spectrum of the zeolite ferrierite. Our results anticipate that ^{17}O NMR measurements combined with high precision DFT calculations will have an important impact in the study of complex systems such as zeolites and silicate glasses.

Appendix

A. Electric Field Gradients with PAW. The EFG tensor $\vec{G}(\mathbf{r})$ can be computed using eq 5, and the total charge density $n(\mathbf{r}) = n^{\mathrm{ION}}(\mathbf{r}) + n^{\mathrm{El}}(\mathbf{r})$, $n^{\mathrm{ION}}(\mathbf{r})$ and $n^{\mathrm{El}}(\mathbf{r})$ being the ionic and electronic charge distributions. To obtain $n^{\mathrm{El}}(\mathbf{r})$, we use a pseudopotential approach and the PAW[7,8] method. The electronic charge density $n^{\mathrm{El}}(\mathbf{r})$ is split into two contributions:

$$n^{\mathrm{El}}(\mathbf{r}') = n^{\mathrm{El,PS}}(\mathbf{r}') + n^{\mathrm{El,corr}}(\mathbf{r}) \quad (9)$$

Here $n^{\mathrm{El,PS}}(\mathbf{r}) = 2\sum_o \langle\tilde{\psi}_o^{(0)}|\mathbf{r}\rangle\langle\mathbf{r}|\tilde{\psi}_o^{(0)}\rangle$ is electronic density calculated from the ground-state pseudo-wave functions $|\tilde{\psi}_o^{(0)}\rangle$. Its contribution to the EFG tensor $G_{\alpha\beta}^{\mathrm{El,PS}}(\mathbf{r})$ can be calculated in reciprocal space from eq 5 with $n(\mathbf{r}) = n^{\mathrm{El,PS}}(\mathbf{r})$. Within PAW, the correction term to the density, $n^{\mathrm{El,corr}}(\mathbf{r})$, is:

$$n^{\mathrm{El,corr}}(\mathbf{r}) = 2\sum_{\mathbf{R},o,J,J'} \langle\tilde{\psi}_o^{(0)}|\tilde{p}_{\mathbf{R},J}\rangle[\langle\phi_{\mathbf{R},J}|\mathbf{r}\rangle\langle\mathbf{r}|\phi_{\mathbf{R},J'}\rangle - \langle\tilde{\phi}_{\mathbf{R},J}|\mathbf{r}\rangle\langle\mathbf{r}|\tilde{\phi}_{\mathbf{R},J'}\rangle]\langle\tilde{p}_{\mathbf{R},J'}|\tilde{\psi}_o^{(0)}\rangle \quad (10)$$

where $|\phi_{\mathrm{R},J}\rangle$ and $|\tilde{\phi}_{\mathrm{R},J}\rangle$ are the all-electron and the pseudopartial-waves of the atomic site **R**. The index $J(J')$ refers to the angular momentum l ($1'$), its projection on the z axis m (m'), and an additional quantum number n (n'). $|\tilde{p}_{\mathbf{R},J}\rangle$ are the projector functions defined in refs 7 and 1 such that $\langle\tilde{p}_{\mathbf{R},J}|\phi_{\mathbf{R}',J'}\rangle = \delta_{\mathbf{R},\mathbf{R}'}\delta_{J,J'}$.

The contribution for the nucleus at **R** of the correction term $G_{\alpha,\beta}^{\mathrm{El,corr}}(\mathbf{R})$ to the EFG tensor can be evaluated from eq 5, setting $n(\mathbf{r}) = n^{\mathrm{El,corr}}(\mathbf{r})$. If we take advantage of the use of norm-conserving pseudopotentials, we can neglect the correction terms due to the density from atomic sites other than **R** to obtain:

$$G_{\alpha\beta}^{\mathrm{El,corr}}(\mathbf{R}) = 2\sum_{o,J,J'} \langle\tilde{\psi}_o^{(0)}|\tilde{p}_{\mathbf{R},J}\rangle\left[\left\langle\phi_{\mathbf{R},J}\left|\frac{1}{r^3}\left[\delta_{\alpha\beta} - 3\frac{r_\alpha r_\beta}{r^2}\right]\right|\phi_{\mathbf{R},J'}\right\rangle - \left\langle\tilde{\phi}_{\mathbf{R},J}\left|\frac{1}{r^3}\left[\delta_{\alpha\beta} - 3\frac{r_\alpha r_\beta}{r^2}\right]\right|\tilde{\phi}_{\mathbf{R},J'}\right\rangle\right]\langle\tilde{p}_{\mathbf{R},J'}|\tilde{\psi}_o^{(0)}\rangle \quad (11)$$

To compute this expression we use the relation $|\phi_{\mathbf{R},J}\rangle = |R_{\mathbf{R},nl}\rangle|Y_{lm}\rangle$, where $|R_{\mathbf{R},nl}\rangle$ is a radial function and $|Y_{lm}\rangle$ a spherical harmonic, so that

$$\left\langle\phi_{\mathbf{R},J}\left|\frac{1}{r^3}\left[\delta_{\alpha\beta} - 3\frac{r_\alpha r_\beta}{r^2}\right]\right|\phi_{\mathbf{R},J'}\right\rangle = \left\langle R_{\mathbf{R},nl}\left|\frac{1}{r^3}\right|R_{\mathbf{R},n'l'}\right\rangle\sum_{m''} c_{m''}^{\alpha\beta}\langle Y_{lm}|Y_{2m''}|Y_{l'm'}\rangle \quad (12)$$

where $\langle Y_{lm} | Y_{2m''} | Y_{l'm'} \rangle$ is a Gaunt integral that can be calculated analytically, and the coefficients $c_{m''}^{\alpha\beta}$, are obtained from the relation:

$$\sum_{m''} c_{m''}^{\alpha\beta} \langle \mathbf{r} | Y_{2m''} \rangle = \delta_{\alpha\beta} - 3\frac{r_\alpha r_\beta}{r^2} \quad (13)$$

If $Z_{\mathbf{R}}$ are the ionic charges, the ionic charge contribution to the EFG is:

$$G_{\alpha\beta}^{\mathrm{ION}}(\mathbf{r}) = \sum_R \frac{Z_{\boldsymbol{R}}}{|\mathbf{r} - \mathbf{R}|^3}\left[\delta_{\alpha\beta} - 3\frac{(r_\alpha - R_\alpha)(r_\beta - R_\beta)}{|\mathbf{r} - \mathbf{R}|^2}\right] \quad (14)$$

This summation is also equal to the β component of the electric field produced by a set of dipoles with dipole moment $Z_{\mathbf{R}}$ oriented along α. It can be calculated exactly within numerical accuracy by an Ewald sum technique.[37]

In Table 6, we validate the EFGs obtained with our DFT implementation against those obtained with an all-electron method, the HF and the second-order Moller−Plesset theory.[38] We use the DFT-GGA with the PBE functional, a supercell of 3000 Bohr^3, and a plane wave energy cutoff of 100 Ry. The cutoff radii for the H, C, 0, F, Cl pseudopotentials are equal to 1.0, 1.6, 1.45, 1.1, and 1.3 Bohr, respectively.

Table 6. Electric Field Gradient Calculations for Small Molecules[a]

	HF	MP2	DFT-PAW
H_2	0.342	0.338	0.337
F_2	6.944	6.258	6.494
HF	0.521	0.546	0.547
H**F**	2.860	2.591	2.757
HCl	0.292	0.296	0.285
HC**l**	3.579	3.402	3.359
CO	−1.174	−0.950	−1.058
C**O**	−0.724	0.779	−0.725
H_2**O** V_{xx}	1.651	1.444	1.524
H_2**O** V_{yy}	−1.836	−1.624	−1.750
H$_2$O V_{bb}	−0.267	−0.271	−0.265
H$_2$O V_{cc}	0.472	0.481	0.471

[a] Comparison of HF and MP2 all-electron calculations[38] with our DFT-PAW results. For dimers we report the largest eigenvalue of the EFG tensor, for the atom in bold. The water molecule is in the (Oxy) plane and the (Ox) axis is a C_2 symmetry axis, the principle axes of the tensor defined as (**a**, **b**, **c**) are chosen so that $|V_{cc}| > |V_{bb}| > |V_{aa}|$ for hydrogen. All values are in atomic units.

Acknowledgment. We thank I. Farnan and D. Padro for providing us with their new experimental ^{17}O parameters of quartz and cristobalite and for useful discussions, and K. A. Peterson for providing us with the cc-pCVxZ basis sets. The calculation have been performed on the IDRIS supercomputer center of the CNRS.

JA027124R

(36) Tossell, J. A.; Lazzeretti, P. *Phys. Chem. Miner.* **1988**, *15*, 564−569.
(37) Honma, A. *Sci. Light* **1976**, *25*, 41.
(38) Bishop, D. M.; Cybulski, S. *M. J. Chem. Phys.* **1994**, *100*, 6628.